Tryptophan Contributions to the Unusual Circular Dichroism of fd Bacteriophage†

Gregory E. Arnold,‡,§ Loren A. Day,‖ and A. Keith Dunker*,‡,§

Department of Biochemistry/Biophysics and Department of Chemistry, Washington State University, Pullman, Washington 99164, Molecular Sciences Research Center, Pacific Northwest Laboratory, Richland, Washington 99352, and The Public Health Research Institute, 455 First Avenue, New York, New York 10016

Received February 28, 1992; Revised Manuscript Received May 26, 1992

ABSTRACT: The circular dichroism (CD) spectrum of fd bacteriophage has a deep minimum at 222 nm characteristic of highly α-helical protein, but there is a shoulder at 208 nm rather than a minimum, with a 222/208-nm amplitude ratio near 1.5 rather than near 1. Oxidation of fd phage with the tryptophan reagent *N*-bromosuccinimide (NBS) changes the ratio. In this report, the NBS titration of fd is followed by CD and three other spectroscopies, the results of which yield an explanation of the unusual CD spectrum. Absorbance, fluorescence, and Raman data show the oxidation to have two phases, the first of which involves the destruction of tryptophan and the second, tryptophan and tyrosine. Raman spectra reveal the invariance of an environmentally-sensitive tyrosine Fermi resonance doublet during the first oxidative phase. Raman spectra also show that little or no change of α-helicity occurs in the first or second oxidation phase, although very slight changes in the helix parameters might be occurring. Concurrent with the destruction of tryptophan during the first phase is the appearance in CD difference spectra ($[\theta]_{\text{NBS-treated fd}} - [\theta]_{\text{native fd}}$) of positive maxima at 208–210 nm and negative maxima at 224 nm, with crossovers at 217 nm. Enormous difference ellipticities, per oxidized subunit of 50 amino acids, of +490 000 ± 80 000 deg cm^2 dmol^{-1} at 208 nm and −520 000 ± 110 000 deg cm^2 dmol^{-1} at 224 nm have been derived from the data. With no apparent change in α-helicity, with no loss of other chromophores, and with the constant nature of the tyrosine environments, the entire spectral change has been assigned to tryptophan. Direct stacking of tryptophan-26 (W26) from one subunit upon phenylalanine-45 (F45) from another subunit, with coupling of the electronic transitions of the two chromophores, is proposed as an explanation of the assigned spectrum.

The filamentous bacteriophage fd (M13, f1; collectively, Ff) has a length close to 900 nm and a diameter between 6 and 9 nm, depending on conditions [reviewed by Makowski (1984), Webster and Lopez (1985), and Day et al. (1988)]. The virus contains 12% single-stranded circular DNA, approximately 1% minor proteins, and 87% major coat protein comprised of 2700 identical copies of a single subunit (Newman et al., 1978; Day et al., 1988). The latter is the product of phage gene VIII, which in its mature form is a single polypeptide chain of only 50 amino acids (pVIII). In the intact phage particle, the pVIII subunit is mostly α-helical (Marvin, 1966; Day, 1966; 1969; Thomas & Murphy, 1975; Tanford & Reynolds, 1976; Williams & Dunker, 1977; Day & Wiseman, 1978; Nozaki et al., 1978; Williams et al., 1980; Thomas et al., 1983; Opella et al., 1987; Clack & Gray, 1989) and is arranged in a closely packed, overlapping manner with its α-helix axis approximately parallel to the main particle axis (Marvin et al., 1974; Makowski & Caspar, 1981; Opella et al., 1987; Marzec & Day, 1988; Day et al., 1988; Marvin, 1990). The resulting capsid is a tight, interlocking network of subunits surrounding the cylindrical core containing the DNA.

The pVIII subunit has charged ends, with 1 basic and 5 acidic residues out of the first 20 at the N-terminus, and with 4 basic residues out of the last 11 at the C-terminus (Asbeck et al., 1969). Between the charged ends, pVIII has 19 consecutive uncharged amino acids (Nakashima & Konigsberg, 1974). Consistent with its amino acid sequence, pVIII is found in the cytoplasmic membrane of the infected cells (Smilowitz et al., 1972; Kuhn, 1990), where it participates in the extrusion and encapsulation of the phage DNA. The membrane-mediated phage assembly/extrusion process occurs without causing cell lysis [reviewed by Marvin and Hohn (1969), Webster and Lopez (1985), Rasched and Oberer (1986), Model and Russel (1988), and Russel (1991)] and may involve the membrane potential (Ng & Dunker, 1981) as well as critical electrostatic interactions (Hunter et al., 1987) and phage- and host-encoded accessory transport proteins (Brissette & Russel, 1990; Russel, 1991; Guy-Caffey et al., 1992).

Compared to the CD spectra of typical water-soluble helical proteins (Greenfield & Fasman, 1969; Chen et al., 1972; Adler et al., 1973), that of the native phage has a highly unusual shape (Nozaki et al., 1976; Day & Wiseman, 1978; Clack & Gray, 1989). The CD spectrum exhibits features of the 208-nm π–π^* and the 222-nm n–π^* electronic transitions that are typical of α-helical conformation, but the amplitudes are anomalous. The 222/208-nm amplitude ratio is about 1.5 for fd as compared to ratios from about 0.85 to about 1.15 for four different helical polypeptides (Adler et al., 1973). While it is known that large assemblies of chromophores, such as viruses, show a variety of distortions in their optical properties as a consequence of being aggregated [reviewed by Tinoco et al. (1980, 1985)], the theory for rodlike particles (Day & Hoppensteadt, 1972) applied to the CD properties

† This work was supported by NIH Grants GM 25937 and GM 25097 awarded to A.K.D. and by NIH Grants AI 09049 and GM 42286 awarded to L.A.D. The Northwest College and University Association for Science Program, funded by Grant DE-AM06-76-RL02225 from the U.S. Department of Energy, provided support for G.E.A. The Pacific Northwest Laboratory is operated for the U.S. Department of Energy by Battelle Memorial Institute under Contract DE-AC06-76RLO 1830.

* Address correspondence to this author at the Department of Biochemistry/Biophysics, Washington State University.

‡ Washington State University.

§ Pacific Northwest Laboratory.

‖ The Public Health Research Institute.

0006-2960/92/0431-7948$03.00/0

of fd does not account for the unusual spectral shape (L. A. Day, unpublished results). Furthermore, other filamentous viruses with essentially the same type of chromophore packing into long rods exhibit normal α-helical CD spectra (Day & Wiseman 1978; Thomas & Day, 1981; Casadevall & Day, 1982; Day et al., 1988; Clack & Gray, 1989). Finally, oxidation of the fd phage with *N*-bromosuccinimide (NBS) causes the 208-nm CD trough to become deeper and the 222-nm trough shallower; the shape of the spectrum of NBS-treated fd approaches that of other α-helical globular proteins and that of Pfl filamentous phage, which lacks the tryptophan (Day & Wiseman, 1978).

Here we present the results of CD, Raman, UV absorbance, and fluorescence studies on the oxidation of the fd phage by NBS, confirming that the anomalous shape of the fd CD spectrum is primarily due to large contributions from tryptophan. Furthermore, we propose a mechanism to account for the unusually large magnitude and atypical shape of the tryptophan contribution.

MATERIALS AND METHODS

Materials. The spectroscopic measurements and the *N*-bromosuccinimide (NBS) oxidations were carried out in 0.01 M borate buffer, pH 8.1, with or without 0.1 M NaCl, which did not seem to markedly affect the results. NBS was purchased from Sigma and recrystallized 3 times from water (mp 180–183 °C). NBS reagent solution was prepared fresh, prior to each experiment, at a concentration of 0.56 mM in 0.1 M NaCl with 0.01 M borate and stored in the dark at 18 °C.

Purification of fd Phage. The fd phage was grown and titrated on *Escherichia coli* CSH 61, from the Cold Spring Harbor collection. After growth on tryptone broth for about 7 h in 20-L New Brunswick fermenters, cells were infected with fd phage. Cells were incubated for an additional 12–16 h (overnight) and subsequently collected by centrifugation (8000*g* for 6 h). The supernatant containing phage was made 0.5 M NaCl and 3% poly(ethylene glycol) (polyethylene glycol 6000 from Sigma) and left 4 days in the cold (4 °C). The supernatant, containing less than 1% of the phage, was siphoned off and discarded. The poly(ethylene glycol)-precipitated phage was redissolved in 0.02 M Tris, pH 8.1, and then subjected to centrifugation at 10000*g* for 2 h to remove cells and debris. The phage was again precipitated with 0.5 M NaCl/3% poly(ethylene glycol) (PEG), then centrifuged at 5000*g* for 1 h, and resuspended in buffer. PEG precipitation cycles were repeated as necessary to obtain phage free of colored material. The final PEG-phase separation was followed by three cycles of differential centrifugation to remove the residual poly(ethylene glycol). The phage was then banded on a preformed KBr density gradient (Fisher ACS certified KBr). The KBr-banded phage was then dialyzed at 4 °C into 0.01 M borate buffer solution, pH 8.1 [see Dunker et al. (1979a)].

Preparation of NBS-Treated Phage. Eight milliliters of fd phage (0.38 mg/mL) was reacted with NBS by addition of incremental aliquots of the NBS reagent solution (0.56 mM). The final volume of the reaction mixture was taken to 10.0 mL by addition of borate buffer. The reaction mixture was then gently stirred in the dark at room temperature (18 °C) for 30 min.

Ultraviolet Absorbance and Circular Dichroism Measurements. Ultraviolet (UV) absorbance spectra were collected on a Perkin-Elmer 320 spectrophotometer driven by a Perkin-Elmer Model 3600 computer datastation following the mixing of reagents and the uniform waiting period of 30 min. Circular dichroism (CD) spectra were then recorded on these samples, diluted 20-fold into 0.1 M NaCl/borate buffer, with a JASCO Model J-40A spectropolarimeter having automatic slit control. The instrument was calibrated with d_{10}-camphorsulfonic acid (Adler et al., 1973) recrystallized from benzene (Krueger & Pschigoda, 1971) with the ellipticity at 210 nm equal to −2.20 deg m^2 mol^{-1}. The sample chamber was flushed with nitrogen, and cell path lengths were either 1 or 10 mm. CD spectra were digitized manually at 0.2-nm intervals with an ALTEK AC40 X,Y coordinate digitizer driven by an IBM-PC/AT microcomputer. The spectra were smoothed using a cubic spline (Savitisky & Golay, 1967). CD difference spectra were generated by subtracting the spectrum for the native phage from each NBS-oxidized fd spectrum. The difference spectra were numerically integrated using the trapezoidal method (Ray, 1975).

Fluorescence Measurements. Fluorescence measurements were made in a 10 mm × 10 mm cuvette at 18 °C with a Perkin-Elmer Model LS-5 fluorescence spectrophotometer. The excitation wavelength was 295 nm, and the band widths for both excitation and emission were set at 2 nm. Measurements were made on 100-fold dilutions of the original phage samples and NBS-treated phage samples, so that fluorescence emission was a linear function of phage concentration.

Raman Scattering Measurements. Raman scattering was excited with a Spectra-Physics Model 16 argon laser (5145 Å), which produced about 100-mW power at the sample. Spectra were collected at 90° relative to the incident laser beam using a Ramanor HG-2S double-slit monochromator and a Spex Digital photometer, under the control of an IBM-PC/XT microcomputer. The spectral slit width was 8 cm^{-1}, and the scan rate was 1 cm^{-1}/s, with an integration time of 1 s. Repetitive scans were averaged, and the base lines were corrected for background fluorescence and then for solvent background by subtraction of the spectrum of water (Williams & Dunker, 1981), and the spectra were smoothed as described by Savitisky and Golay (1967). The samples consisted of concentrated solutions of phage or NBS-treated phage, at concentrations near 150 mg/mL, in borate buffer. These samples were prepared by subjecting the original phage and NBS-treated phage to high-speed centrifugation for 12 h at 25000*g* and 4 °C and transferring the wet pellets to capillary tubes. The capillaries were sealed, and maintained at 21 ± 0.5 °C in a water-jacketed sample holder for the measurements.

RESULTS

UV Absorbance and Fluorescence Studies. If the contributions from the minor capsid proteins are ignored because they comprise only about 1% of the total proteins, then the absorbance spectrum of fd phage (Day, 1969) from 240 to 350 nm is the sum of contributions from the following chromophores (per mole of pVIII subunit): 1 Trp, 2 Tyr, 3 Phe, and 2.3–2.4 nucleotide bases (25% A, 34% T, 21% G, 20% C). The absorbance spectrum and changes in it produced by NBS oxidation are shown in Figure 1. With increasing amounts of NBS, there is a monotonic decrease in absorbance at 280 nm, monotonic increases near 245 and 310 nm, and invariant points at 260 and 295 nm. In difference spectra (not shown), a slight red-shift of a 280-nm peak, a blue-shift of the 245-nm trough, and the formation of a shoulder around 300 nm can be discerned. All of these changes in absorbance are typical of NBS oxidation of tryptophan to an oxindole derivative (Patchornik et al., 1958; Spande & Witkop, 1967). A difficulty encountered was the development of increasing amounts of

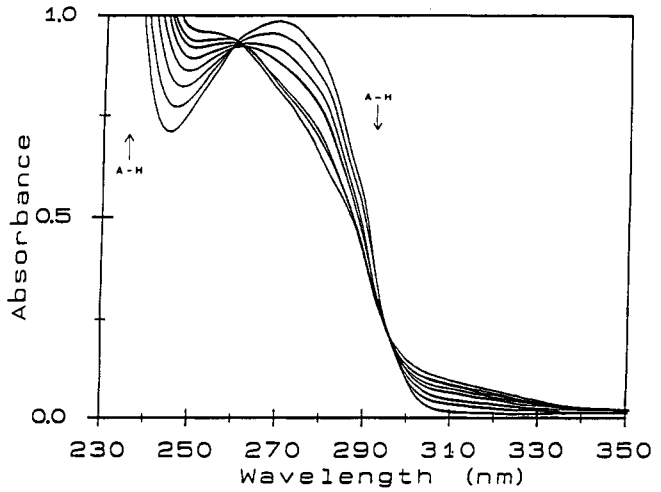

FIGURE 1: Absorption spectra of the fd phage as a function of increasing NBS/tryptophan mole ratios. Aliquots of NBS (0.56 mM stock solution) were added to 8 mL of fd solution and taken to a final volume of 10 mL using borate buffer solution; the spectra were collected at 18 °C. The spectra are for the following NBS tryptophan ratios: (A) 0.0 (uppermost spectrum at 270 nm, lowermost at 250 and 310 nm); (B) 0.3; (C) 0.5; (D) 0.8; (E) 1.2; (F) 1.6; (G) 2.4; (H) 3.4 (lowermost spectrum at 270 nm, uppermost at 250 and 310 nm).

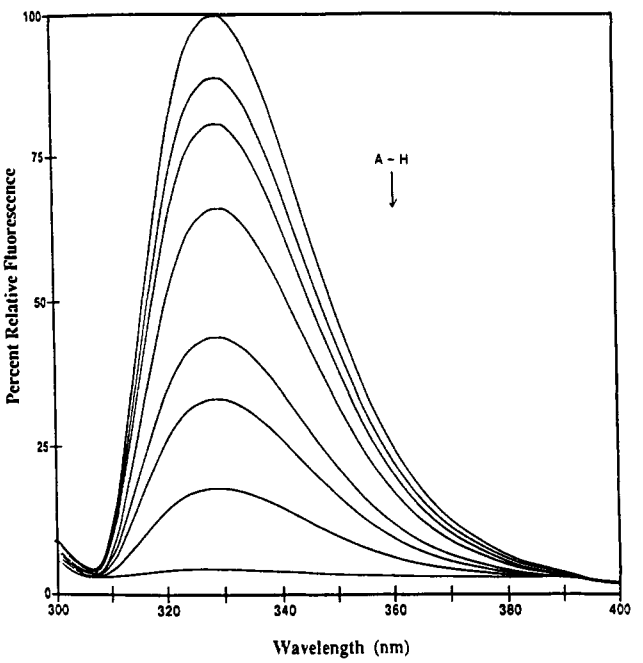

FIGURE 2: Reduction of fd fluorescence by oxidation with NBS. Aliquots of NBS (0.56 mM stock solution) were added to 8 mL of fd solution and taken to a final volume of 10 mL. The phage/NBS solution was then diluted 100-fold using borate buffer solution, and the spectra were recorded after excitation a 295 nm, 18 °C. The indicated spectra are for the following NBS/tryptophan ratios: (A) 0.0; (B) 0.3; (C) 0.5; (D) 0.8; (E) 1.2; (F) 1.6; (G) 2.4; (H) 3.4.

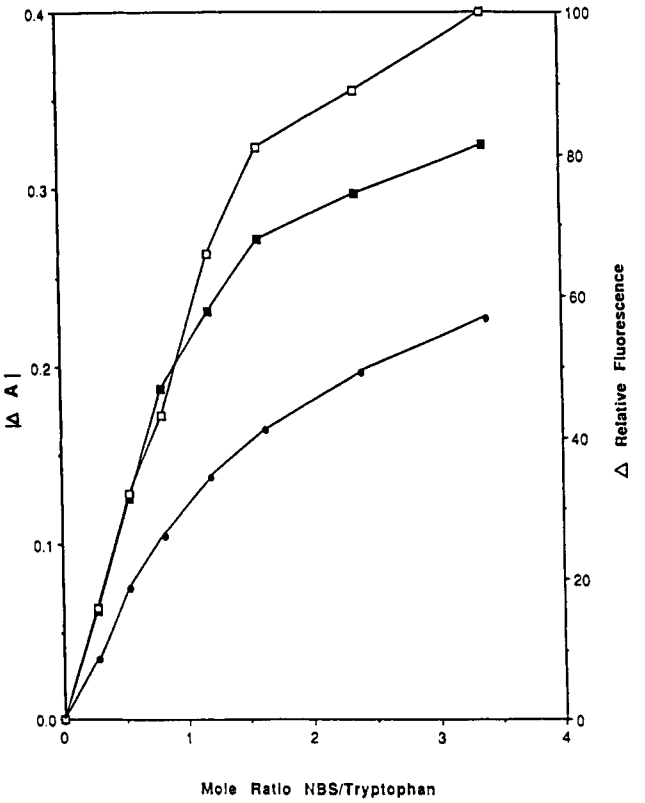

FIGURE 3: Effects on absorbance and fluorescence for fd phage with increasing NBS/tryptophan ratios. Data from Figures 1 and 2 are plotted here so increases and decreases can be more easily compared. The left ordinate represents the absolute change in absorption [at 245 (□) and 280 nm (●) the right ordinate represents the change in relative fluorescence intensity [at 329 nm (□)] and is plotted as functions of NBS/tryptophan mole ratios.

turbidity at NBS/pVIII mole ratios greater than about 2/1; eventually, there was precipitation of the sample at ratios greater than about 4/1 which prevented the determination of titration end points. The turbidity stems from oxidation byproducts caused by NBS side reactions, or from cleavage of the protein backbone at the tryptophan moiety as described previously for other proteins (Creed, 1984). Cleavage could cause a gross structural change in pVIII, and could account for precipitation of the oxidized phage solution; precipitation has been observed for NBS titrations of other proteins (Spande & Witkop, 1967). Spectra in Figure 1 at mole ratios greater than 1 have modest corrections for light scattering that were determined by log absorbance versus log λ plots.

Native fd exhibits an intense fluorescence emission maximum at 330 nm when excited at 280 nm (Day et al., 1979), and excitation at 295 nm produces a similar emission spectrum (Figure 2). We chose 295 nm to monitor the effects of NBS on the virus fluorescence (Figure 2) because there is no discernible change in absorbance at this wavelength at low mole ratios of added NBS (Figure 1) and because the extinction coefficient of tryptophan at 295 nm is more than 100 times that of protonated tyrosine. Increments of NBS cause progressive reduction of the emission intensity, and at an NBS/tryptophan mole ratio of 3.4/1, emission is almost totally eliminated. There is a slight red-shift in the approximate maximum of emission from 329 nm, for native phage, to 333 nm, for the NBS-treated phage. The UV and fluorescence changes are compared in Figure 3, which gives the absolute values of the UV and fluorescence changes discussed above. The decrease in fluorescence emission at 329 nm parallels the decrease in UV absorption at 280 nm and the increase at 245 nm. The plots for changes in fluorescence and in 245-nm absorbance both indicate a slope change near the 1.6 NBS/subunit ratio, whereas the plot for changes in 280-nm absorbance does not.

Raman Scattering. Raman spectra in the frequency region from 600 to 1800 cm^{-1} at increasing NBS/subunit mole ratios are shown in Figure 4. The sharp amide I band at 1649 cm^{-1} is indicative of a very high helix content (Lord & Yu, 1970; Franconi et al., 1970; Thomas & Murphy, 1975; Williams & Dunker, 1981; Thomas et al., 1983; Thomas, 1988). In Figure 4, it can be seen that amide I at 1649 cm^{-1} remains invariant

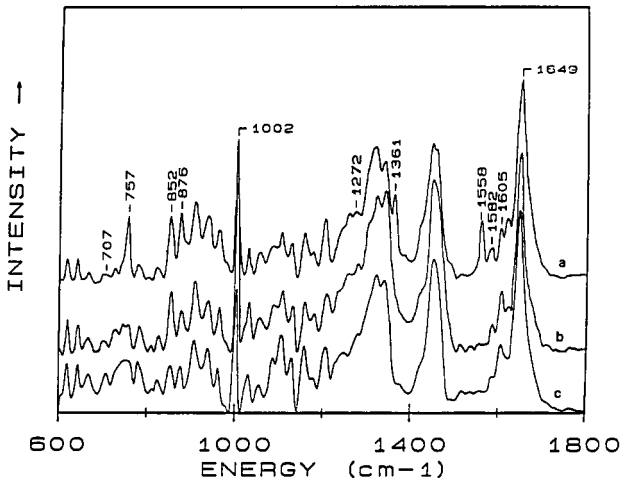

FIGURE 4: Raman spectra of fd phage, at ~150 mg/mL, in 0.01 M borate buffer solution, pH 8.1, 21 °C. Spectra were excited with 100 mW of 5145-Å radiation and recorded at a scan rate of 1 cm^{-1}/s and a slit width of 10 cm^{-1}. The spectra are (a) native fd phage, (b) NBS-treated fd phage with a 1.2 NBS/tryptophan mole ratio, and (c) NBS-treated fd phage with a 3.4 NBS/tryptophan mole ratio.

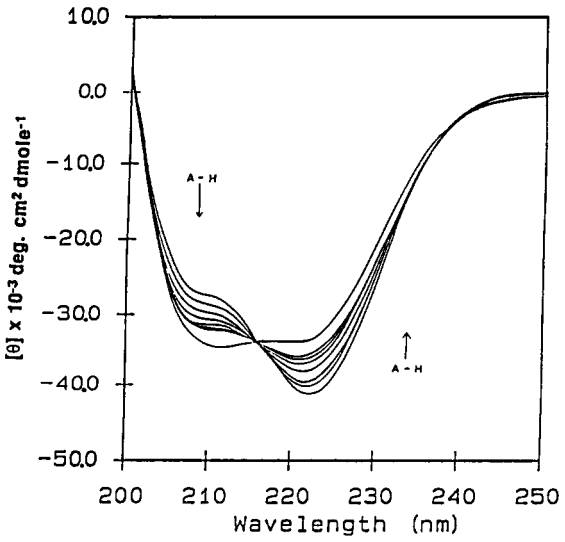

FIGURE 5: Effect on ellipticity at specific wavelengths in the circular dichroism spectra of the fd phage with increasing NBS/tryptophan ratios: (A) 0.0; (B) 0.3; (C) 0.5; (D) 0.8; (E) 1.2; (F) 1.6; (G) 2.4; (H) 3.4.

up to and including the highest NBS/pVIII mole ratio tested, indicating that the amount of α-helix in pVIII does not change during NBS oxidation.

The amide III region from 1270 to 1310 cm^{-1} has previously been assigned to helical structure (Lord & Yu, 1970; Franconi et al., 1970; Yu, 1977). In fd, this spectral region is complex, with amide III bands at about 1313, 1302, and 1270 cm^{-1} being distinguished by means of their different rates of deuterium exchange (Williams et al., 1984); in addition, this region contains substantial intensity from other bands as judged from the considerable intensity remaining after complete deuterium exchange (Williams et al., 1984). Thus, it is difficult to interpret the slight changes in band shape that occur in the 1260–1320 cm^{-1} region with NBS oxidation.

The Raman bands that have been previously shown to be due to indole ring vibrations, including those at 757, 876, 1337, 1361, 1558, and 1582 cm^{-1} (Thomas et al., 1983; Aubrey & Thomas, 1992), are greatly diminished at 1.2 mol of NBS/mol of pVIII; some additional change in these peaks may also occur when NBS is raised to 3.4 mol of NBS/mol of pVIII (Figure 4). These tryptophan-specific spectral changes are comparable to those observed in the Raman spectra obtained for NBS oxidation of the tryptophan-rich protein lysozyme (Schmidt & Bieker, 1979). In spectra 4b and 4c, new low-intensity scattering signals can be discerned at 667 and 708 cm^{-1} together with new shoulders at 761 and 1018 cm^{-1}. These correspond to Raman scattering from the oxindole product resulting from NBS oxidation of tryptophan (Schmidt & Bieker, 1979). Comparison of spectra 4a, 4b, and 4c shows a loss in intensity of the 1617-cm^{-1} Raman peak, most of which parallels the loss in intensity of the tryptophan bands at 757, 1361, and 1558 cm^{-1} following the addition of 1.2 mol of NBS/mol of pVIII. These data indicate significant tryptophan contribution to the intensity at 1617 cm^{-1}, although the tyrosines probably also contribute to this band as assigned previously (Thomas et al., 1983; Aubrey & Thomas, 1991). Contributions from both tryptophan and tyrosine for the 1617-cm^{-1} peak are supported by the early investigations of the Raman scattering from the various amino acids (Lord & Yu, 1970).

The tyrosine Fermi resonance doublet near 850 and 830 cm^{-1} shows little or no change in spectrum 4b as compared to 4a, but becomes markedly altered in 4c. Using the nomenclature described previously (Siamwiza et al., 1975), the I_{850}/I_{830} ratio is near 10/2.7 in 4b, which is the value reported for fd phage (Dunker et al., 1979b; Thomas et al., 1983), but changes to about 10/5.5 in 4c. Since this ratio is very sensitive to the hydrogen-bonded state of the tyrosine (Siamwiza et al., 1975; Dunker et al., 1979a,b), these data strongly indicate that there is no change in the environments of the two tyrosines up to about 1.2 mol of NBS/mol of pVIII.

Oxidation Takes Place in Two Phases or Steps. The first oxidative step is characterized by a decrease in fluorescence intensity at 329 nm and an increase in UV absorbance at 245 nm; both are consistent with the oxidation of tryptophan. In the Raman spectrum at an NBS/pVIII mole ratio of 1.2 (Figure 4b), tryptophan bands have been reduced almost completely, but tyrosine bands are preserved with little or no change, including essentially no change in the environmentally-sensitive Fermi resonance doublet near 850 and 830 cm^{-1}. The change in slope near 1.6 mol of NBS/mol of pVIII in the fluorescence and 245-nm absorbance curves (Figure 3) defines the beginning of the second step. In the Raman spectrum for the most extensively NBS-oxidized phage sample (Figure 4c), the oxidation of tyrosine is evident as indicated from the diminished intensity of the 852-cm^{-1} phenolic ring vibration and from the change in the I_{850}/I_{830} ratio.

Changes in the Anomalous CD. Circular dichroic changes brought about the NBS titration of fd are shown in Figure 5. Incremental addition of NBS causes a concomitant decrease in the negative ellipticity at 222 nm and an increase in the negative ellipticity at 208 nm (Figure 5). At the highest NBS concentration used, the 208- and 222-nm troughs become nearly equal. Both of these troughs exhibit a small but progressive blue-shift throughout the titration profiles.

The same data displayed as CD difference spectra ($[\theta]_{\text{NBS-treated fd}} - [\theta]_{\text{native fd}}$) are shown in Figure 6. The difference spectra exhibit positive and negative lobes at 208–210 and 224 nm, respectively, and the crossover at 217 nm. Increments of NBS initially cause large simultaneous gains in amplitude in both lobes, indicating an intimate association of these two dichroic bands. The changes become small for NBS/pVIII mole ratios of 1.2, 1.6, and 2.4. This region of slow change in the CD spectra corresponds approximately with the regions of lower slopes observed in the fluorescence

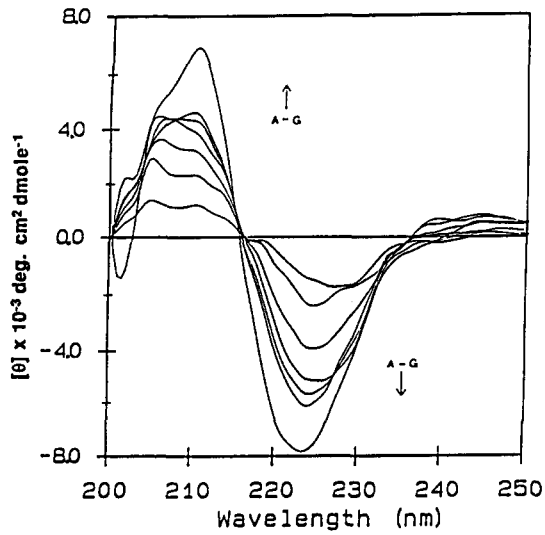

FIGURE 6: Circular dichroism difference spectra. These difference spectra were obtained by subtracting the spectrum of native fd phage from each of the NBS-treated phage spectra (Figure 5). The spectra correspond to the following NBS/tryptophan ratios: (A) 0.0 (base line); (B) 0.3; (C) 0.5; (D) 0.8; (E) 1.2; (F) 1.6; (G) 2.4; (H) 3.4.

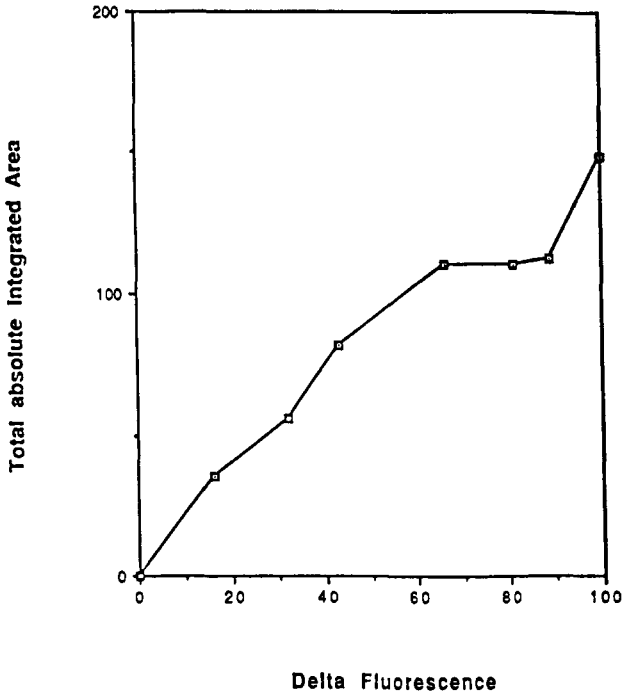

FIGURE 7: Comparison of changes in the difference spectra with changes in fluorescence. The summed absolute values of the two lobes of difference spectra (Table I) are plotted against the changes in fluorescence as determined from Figure 2.

and 245-nm absorbance plots (Figure 3). The area bounded by the negative lobe is somewhat greater than that of the positive lobe.

CD of Tryptophan in Native fd Phage. The destruction of tryptophan by NBS oxidation, as monitored by absorbance, fluorescence, and Raman spectroscopies, is accompanied by the concurrent positive and negative changes in the CD spectrum (Figures 5 and 6), but without any apparent loss of α-helicity. To further test whether the loss of tryptophan is responsible for the CD spectral changes, the absolute values of the integrated areas of the difference CD spectra are plotted against the fractional change in the fluorescence intensity (Figure 7). The initial, approximately linear portion of this plot and the Raman data for NBS/pVIII mole ratios up to 1.2, indicating destruction of tryptophan yet no other changes, especially no apparent changes in α-helicity or in the tyrosine Fermi resonance doublet, show that the difference CD spectra are primarily due to tryptophan. Given this assignment of all the change to a single residue, the difference spectra in Figure 6 can be expressed per mole of pVIII molecule (or per tryptophan) rather than per peptide linkage (49 per pVIII). We then calculate, for each increment of NBS, a CD spectrum for the tryptophan in the native phage by simply rescaling each CD difference spectrum to the fraction of tryptophan oxidized to that point in the titration, based on the fraction of total fluorescence that has been lost. The data up to 1.2 mol of NBS/mol of pVIII give +490 000 ± 80 000 deg cm^2 dmol^{-1} for the peak at 210 nm and −520 000 ± 110 000 deg cm^2 dmol^{-1} for the trough at 224 nm (Table I).

Table I: Estimation of Tryptophan Ellipticities

CD difference spectrum	fraction of tryptophan oxidized[a]	tryptophan ellipticity (×10^{-3}) at 208 nm[b]	tryptophan ellipticity (×10^{-3}) at 224 nm
a	0.16	+530	−660
b	0.31	+570	−420
c	0.47	+480	−550
d	0.58	+385	−440
		av +490 ± 80	−520 ± 110

[a] Fraction tryptophan oxidized was estimated as $1 - F_i/F_o$, where F_i is the fluorescence at 329 nm of the ith increment of NBS and F_o is the initial fluorescence of fd (Figures 2 and 3). [b] Molar tryptophan ellipticities = (mean residue ellipticity)(49)/(fraction tryptophan oxidized). There are 49 peptide bonds and only 1 tryptophan per subunit. Units are degrees centimeter squared per decimole.

DISCUSSION

NBS Oxidation of fd Phage. Taken together, the UV, Raman, and fluorescence spectroscopy experiments show the progressive destruction of tryptophan (W26) upon incremental addition of NBS. This is evident from the serial changes in absorbance at 245, 280, and 300 nm (Figures 1 and 3) accompanied by the concurrent loss of fluorescence intensity at 330 nm (Figures 2 and 3). The formation of an oxindole product is detected by its strong absorption band at about 245 nm, by its significantly weaker absorption band near 290 nm (Green & Witkop, 1964), and by its weak Raman peaks at 667, 708, 761, and 1018 cm^{-1} (Schmidt & Bieker, 1979). Tyrosine bands become affected at high NBS/pVIII ratios, but products have not been assigned. The phenylalanine Raman peak at 1002 cm^{-1} remains unaffected at all NBS/pVIII ratios tested. It is unclear whether NBS oxidizes the methionine residue (M28), since there are no significant Raman bands or UV absorbance or fluorescence signals for this amino acid over the spectral ranges examined.

The tryptophan is highly accessible to the NBS reagent. The low NBS/pVIII mole ratio needed to oxidize it places it among the most easily oxidized tryptophans studied by this technique (Green & Witkop, 1964; Spande & Witkop, 1967). Recent studies of the Raman spectra of fd with deuterated tryptophan residues have revealed that the tryptophan is in a hydrophilic environment (Aubrey & Thomas, 1992), yet earlier fluorescence data show a low wavelength for the emission maximum and a very high quantum yield, characteristics normally described to tryptophans rigidly held in hydrophobic environments. Nuclear magnetic resonance (NMR) data show that the tryptophans are immobile on millisecond time scales (Gall et al., 1981, 1982; Cross & Opella, 1982, 1983, 1985), which is consistent with the type of

environment inferred from the fluorescence data. Thus, Raman data and NBS oxidation suggest that the tryptophan is "exposed" whereas fluorescence and NMR suggest that it is "buried". We suggest the tryptophans are therefore partially buried and immobilized, but with sufficient exposure to account for the Raman data and ease of oxidation by NBS.

The NBS titration begins with what appears to be specific tryptophan oxidation and then shifts to a mixture of tryptophan and tyrosine oxidation. Evidently, as tryptophans become oxidized, tyrosine can compete more effectively for the NBS. Raman studies indicate that the tyrosyl OH groups are inaccessible to the solvent (Dunker et al., 1979b; Thomas et al., 1983). Consistent with the Raman data, UV spectrophotometric and NMR pH titrations show the tyrosyl OH groups to remain protonated up to pH 12, above which phage disruption and tyrosine deprotonation both occur (Dunker et al., 1979b; Cross & Opella, 1981). Thus, the virtual exclusive oxidation of tryptophan during the first step might be aided by an inaccessibility of the tyrosines.

The doublet tyrosine peaks near 850 and 830 cm^{-1} are due to Fermi resonance between a ring-breathing vibration and an overtone of an out-of-plane ring-bending vibration (Siamwiza et al., 1975). In model compounds, the I_{850}/I_{830} ratio varies from about 10/4 (if the tyrosyl OH is the acceptor of a strong hydrogen bond) to about 3/10 (if the tyrosyl OH is the donor of a strong hydrogen bond). In fd, this ratio is near 10/2.7, indicating that both tyrosines are the recipients of hydrogen bonds from very acidic donors (Dunker et al., 1979a,b; Thomas et al., 1983). Since this value is such an extreme, being even smaller than the value of the most extreme model compound used in the original study, this ratio is a very sensitive indicator of the local tyrosine environment; as shown previously, even slight perturbations of the capsid structure are registered by changes in this ratio (Dunker et al., 1979a,b). Up to 1.2 mol of NBS/mol of pVIII, this ratio is, within experimental error, identical to the 10/2.7 observed for fd phage (Figure 4b), suggesting no detectable change in the tyrosine environment during this step. During the second oxidative step, this ratio changes to about 10/5.5, indicating an alteration in the environments of the remaining, unoxidized tyrosines. Tyrosines in aqueous solution show a ratio near 10/8 (Siamwiza et al., 1975); thus, the direction of the change, from about 10/2.7 to about 10/5.5, suggests that the environments of the tyrosyl OHs become more waterlike during the second oxidation step.

Explanation of the CD Changes. CD spectra are the sum of all contributing chromophores which, in the case of the 200–250-nm region for fd, consist of 49 backbone peptide chromophores, 2 side-chain amide groups, 1 tryptophan, 2 tyrosines, 3 phenylalanines, and 2.3–2.4 nucleotide bases for every 1 of the 2700 subunits in the virus particle. Superimposed on individual contributions are those from differential scattering of the left and right circularly polarized light and absorbance flattening effects. Minor perturbations of subunit packing due to experimental conditions could cause changes in any of these chromophores leading to variations in the 224/208-nm ratio. Different published CD spectra of fd phage exhibit considerable variation in the 222/208-nm ratio, from about 1.4 to 1.54. The strong phenylalanine Raman peak near 1002 cm^{-1} in the fd phage spectrum has been shown to exhibit ionic strength-dependent hypochromism (Thomas et al., 1983), indicating that the subunit packing may be sensitive to ionic strength. Finally, pH changes might also be expected to affect the 222/208-nm ratio. Initial experiments suggest that temperature, pH, and ionic strength can all affect the 222/208-nm ratio in the CD spectra of fd phage and thus variations in these parameters may account for some of the differences in the published spectra. DNA contributions in this region are relatively small as shown in the original ORD study (Day, 1966), but could have small modifying effects.

Oxidation of the tryptophan could lead to structural perturbations that change the amount of helix, which in turn would alter the CD spectrum by indirect effects. However, the strong Raman amide I vibration at 1649 cm^{-1} remains constant in both peak wavelength and intensity (relative to the phenylalanine marker at 1002 cm^{-1}), regardless of the NBS concentration used. The slight changes in the amide III region from 1240 to 1320 cm^{-1} could be due to changes in other bands, such as CH_2 deformations [e.g., see Thomas et al. (1983) and Williams et al. (1984)], or could be due to very subtle alterations in the helical parameters. The differences in this region during the first oxidative step, e.g., Figure 4a compared to 4b, are comparable to changes observed as a result of variations in ionic strength [compare with data in Thomas et al. (1983)]. Thus, when combined with the invariance of the amide I peak, the Raman data in the 1240–1320-cm^{-1} region suggest no changes in helix structure, or at most, these data admit the possibility of only very subtle changes in the helical parameters.

Manning and Woody (1991) recently carried out theoretical studies on the expected CD spectra for α- and 3-10 helices with different choices of the Φ and Ψ angles. The major effect of changing the helical parameters appears to be coordinate increases or decreases throughout the 200–250-nm region. However, the calculations are not sufficiently refined to yield the characteristic double minima near 208 and 222 nm for the α-helix, giving instead a broad single minimum in this region. Furthermore, hydrogen bonding to the amide carbonyl could be involved in stabilizing some of the helical geometries with tilted peptide bonds (Blundell et al., 1983), and such hydrogen bonding, which was not included in the calculations, could markedly affect the results. Another type of subtle change is suggested by further calculations (Cooper & Woody, 1990) showing somewhat different spectra for coiled-coil and straight helices, the change in going from coiled to straight being similar in shape to the changes between native and oxidized fd. Another subtle change has been observed upon the transfer of α-helical polypeptides from water to nonaqueous solvents like trifluoroethanol (Quadrifoglio & Urry, 1969), again yielding spectral changes of the same shape as reported here. Thus, overall the possibility remains that indirect structural changes in helical parameters induced by oxidation of tryptophan could be contributing to the observed spectral changes, but in view of the invariance of the amide I band, we expect that the possible indirect effects probably make second-order contributions.

Both tryptophan and tyrosine have an absorption band near 225 nm, one of the two regions of large change in the CD spectrum; thus, tyrosine is the best alternative candidate to account for the observed spectral changes. The obvious reduction of the tyrosine Raman band at 852 cm^{-1} during the second oxidative step is accompanied by a substantial change in the Fermi resonance doublet at 850 and 830 cm^{-1}; the I_{850}/I_{830} ratio changes from about 10/2.7 to about 10/5.5 (Figure 4b,c). Apparently, the oxidation of some of the tyrosines is accompanied by a perturbation of the environment of the remaining tyrosine. Since the two tyrosines are located at positions 21 and 24, they are probably interacting with each other on one side of the pVIII helix; oxidation of one could lead directly to a perturbation of the environment of the other.

Therefore, the apparent invariance of the I_{850}/I_{830} ratio over the first oxidative step provides strong evidence that no tyrosine oxidation occurs and, furthermore, that no environmental perturbation occurs either, during the first step. Thus, environmental changes or loss of tyrosine almost certainly does not contribute to the CD spectral changes observed during the first oxidative step.

CD for the Tryptophan in Native fd. We have presented under Results a spectrum for the tryptophan in fd virus (Figure 6, Table I). This spectrum is actually a derived result, based on an analysis of four types of spectral data, all gathered as a function of added NBS reagent. The lack of substantial contributions from the backbone and from tyrosine (previous section, above) and the direct correlation between the CD spectral change and the loss of tryptophan fluorescence (Figure 7) combine to suggest that the spectral changes are, to a first approximation, due solely to tryptophan.

The derived tryptophan CD spectrum differs markedly in shape, sign, and amplitude from the *N*-acetyl-L-tryptophanamide CD spectrum (Adler et al., 1973). The amplitudes given in Table I are about 40 times larger than those for the tryptophan model compound. A mechanism involving coupled oscillators might be responsible for these large-scale changes in the tryptophan CD spectrum. The CD difference spectra in this range exhibit the characteristic shape of coupled oscillators with positive and negative lobes, with concomitant appearance of the two lobes (Figure 6). Such coupling is the mechanism underlying the CD spectra of the stacked bases in nucleic acids, and the requirements for coupling are that the chromophores be close in three-dimensional space and close in energy (Tinoco et al., 1963, 1980).

For the tryptophan of fd, prospective coupling partners are those with strong transitions near 217 nm, and these include tryptophan from another subunit, tyrosines and phenylalanines from the same or other subunits, backbone or side-chain amides, or several of the DNA bases. At a given axial position, such as the level of W26, each subunit is in potential contact with five other subunits and the DNA. Tryptophan interactions with DNA seem unlikely in that the absorbance and CD properties of the DNA can be explained in terms of base–base stacking of the DNA in the interior of the virus (Day, 1969; Casadevall & Day, 1982, 1983). The amino acids of the neighbors having approximately the same Z coordinate along the main structure axis as W26 of a "zeroth" reference subunit can be deduced from the lattice diagram [Makowski & Caspar, 1981; see also Marvin (1989, 1990)] and the overall shape of the extended α-helical subunit, which was suggested by Marvin and Wachtel (1975, 1976) and established unequivocally in remarkable experiments by Opella et al. (1987). At a displacement of −32.2 Å is D4 or D5 of subunit −11, at −16.1 Å is Q15 of subunit −6, at +16.1 Å are T36 and I37 of subunit +6, and at +32.2 Å is S47 of subunit +11 and also nearby is F45 of subunit +11 (see Figure 8).

Of the various possibilities given above, coupling between F45 of subunit +11 and W26 of subunit 0 is proposed as the most likely explanation of the derived CD spectrum for tryptophan. First, F45 of subunit +11 is probably the closest geometrically; F45 could be within 3 Å axially of W26, a distance encompassed by the thickness of an aromatic stack. Second, phenylalanine has a strong absorption band near 210 nm; oscillator coupling between this 210-nm band and the 225-nm band of tryptophan provides a simple explanation of the observed spectrum. Recent calculations of possible rotational strengths of a tryptophan–phenylalanine stacked

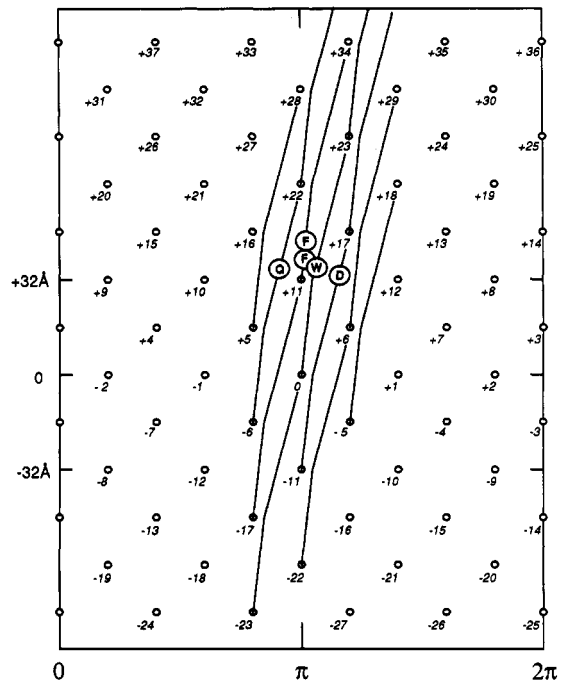

FIGURE 8: Lattice diagram of fd relating the azimuthal and *z*-axis coordinates of equivalent positions of the subunits. The purpose of this diagram, which is adapted from the lattice of Makowski and Caspar (1981) [see also Marvin (1989, 1990)], is to demonstrate the probable close spacing, in the axial direction, between W26 of the zeroth subunit and F42 and F45 of subunit +11 as well as D4 (and D5) of subunit −11 and Q15 of subunit −6. Individual subunits are represented as bent lines which correspond to axes of α-helices which gently curve around the main structure axis. It should also be kept in mind that the α-helical subunits vary radially in the capsid and overlap like shingles on a roof, but that these aspects of subunit packing are not depicted here. The overall shape of the subunit is known from NMR (Opella et al., 1987), but the mutual arrangement of subunits and the proposed side-chain interactions in the lattice (Marvin, 1990) are not yet established [the near-equivalence of representations in lattice diagrams of various detailed models has been discussed (Marzec & Day, 1988)]. The subunit numbers [see Marvin (1989)] have been placed near the C-termini, and the overall length of the subunit axis is 75 Å, corresponding to 1.5 Å for each of its 50 amino acids. The residue positions run from top to bottom, with residue 50 of a given subunit close to the identifying number for that subunit. The sequence is AEGDDPAKAAFDSLQASATEYIGYAWAMVVVIVGATIGIKLFKKFTSKAS.

pair as a function of orientation angle indicate that their transitions can indeed couple to yield the characteristic positive and negative lobes, each having molar ellipticities of about 2 × 10^5 deg cm^2 dmol^{-1} (R. W. Woody, personal communication). Third, the CD spectra of related viruses If1 and IKe, viruses which have W and F residues in exactly the same relative positions as in fd, show very similar-shaped initial CD spectra (Day et al., 1988) and very similar effects upon NBS oxidation (L. A. Day and R. L. Wiseman, unpublished results); in contrast, the Pf1, Pf3, and Xf filamentous phages, which lack equivalently positioned chromophores, yield CD spectra typical of α-helical proteins (Day et al., 1988). Fourth, chloroform-induced contraction of fd phage to short rod- and spherical-shaped particles (Griffth et al., 1981) leads to CD spectra which are like those for highly helical proteins, without the distortion under discussion here [see Dunker et al. (1991a,b)]; in these contracted structures, none of the chromophores have been altered covalently. Given these observations, we propose that the observed tryptophan contribution to the fd CD spectrum in the 200–250-nm region is due, wholly or in large measure, to electronic coupling between W26 on one subunit and F45 on a neighboring subunit; the large

magnitude of the derived CD spectrum implies that these two side chains are in van der Waals contact in the capsid.

Previous Interpretations. The optical absorbance phenomena of bunches of chromophores in large particles are distorted relative to the same absorbance phenomena of the same chromophores uniformly dispersed in solutions, and the magnitudes of possible effects have been estimated for particles of different shapes and sizes (Duysens 1956; Schneider, 1970; Day & Hoppensteadt, 1972; Gitter-Amir, 1975; Tinoco et al. 1980, 1987). In the absence of explicit calculations for the filamentous phage for which the treatment for rods is a good first approximation (Day & Hoppensteadt, 1972), Nozaki et al. (1978) attributed the unusual CD intensity distribution in fd to optical distortions. However, detailed calculations suggested that the optical distortions arising from a cylindrical or rodlike particle would probably not be sufficient to account for the unusual spectrum (L. A. Day, unpublished results), and other filamentous viruses such as Pfl, Xf, and Pf3 exhibit normal CD spectra (Day & Wiseman, 1978; Thomas & Day, 1981; Casadevall & Day, 1983; Clack & Gray, 1989). In view of these results, the unusual fd spectrum has remained unexplained. The observation of Day and Wiseman (1978) pointed to the current experiments.

Recently, Clack and Gray (1989) attempted to analyze the CD spectrum of native fd to determine the α-helix content of its major coat protein. Using the reference set of Greenfield and Fasman (1969), they found an α-helix content of 88 ± 5%, but the fd spectrum was poorly fit. They added an explicit tryptophan contribution to the Greenfield and Fasman reference set; since the CD spectrum of *N*-acetyl-L-tryptophan is actually negative below 220 nm whereas a positive contribution was needed, Clack and Gray (1989) multiplied the tryptophan spectrum by −1 before adding it to the reference set, since rotation of the asymmetrical indole side chain of tryptophan could reverse the sign of the CD spectrum (Woody, 1985), and obtained a somewhat improved fit to the native spectrum and an estimated α-helix content of 98 ± 2% (Clack & Gray, 1989). Because of the residual uncertainties about contributions from tryptophan and its interactions, as well as from other sources, we prefer to estimate the α-helix content simply as >90%.

Implications with Regard to CD Studies of Other Proteins. It is well-known that different helical proteins exhibit different 222/208-nm ratios [for example, see Chen et al. (1972) and Alder et al. (1973)] that also differ from the ratios of helical models, such as poly(L-lysine) which lack the chromophoric side chains. The 222/208-nm variations have long been attributed to side-chain chromophore contributions (Hooker & Schellman, 1970; Chen & Woody, 1971), which are known to become especially pronounced in systems where the aromatic groups are in close proximity (Manning & Woody, 1989), but our present data reveal new aspects with regard to the possible wavelengths and amplitudes of these contributions. The tryptophan, phenylalanine, and tyrosine side chains inside proteins are more often than not found to be in interacting pairs and clusters (Warme & Morgan, 1978). These interacting chromophores exhibit a range of dihedral angles and distances (Burley & Petsko, 1985; Singh & Thornton, 1985), so that chromophore coupling, if present, would be expected to vary. The enormous values deduced here, on the order of 10^5 deg cm^2 dmol^{-1}, exceed by an order of magnitude the conformationally sensitive amplitudes for the backbone peptide chromophore. Obviously, such large side-chain contributions lead to uncertainties in the use of CD spectra to estimate protein secondary structure [see also Manning and Woody (1989)].

On the other hand, in favorable circumstances, the large signals from oscillator coupling may provide important information about the interactions between the side-chain chromophores. For example, recent stopped-flow circular dichroism investigations of early events in the folding of dihydrofolate reductase reveal a signal like those due to coupled oscillators (Kuwajima et al., 1991); the transient has a trough at 220 nm, a peak at 230 nm, and a crossover near 225 nm. The three-dimensional structure of this protein points to a particular tryptophan/tryptophan pair, and this possibility is supported by the CD spectral changes that accompany the elimination of either tryptophan using site-directed mutagenesis (Kuwajima et al., 1991; B. Jones and C. R. Matthews, personal communication). In general, pairwise or multiple coupling between any of the aromatic or other side-chain chromophores could lead to substantial effects in the 200–250-nm region. Through a variety of advances in instrumentation and molecular genetic techniques, it has become possible to test specific hypotheses by examining the CD spectra for proteins and their mutants of known structure having altered side-chain chromophore interactions.

ACKNOWLEDGMENT

We thank R. Foster and R. W. Woody for helpful discussions with respect to the interpretations of the CD data, and T. Cross, L. Makowski, D. A. Marvin, and G. J. Thomas, Jr., for discussions of other aspects.

REFERENCES

Adler, J. T., Greenfield, N. J., & Fasman, G. D. (1973) *Methods Enzymol. 27*, 675–735.
Asbeck, F., Beyreuther, K., Kohler, H., Wettstein, G., & Braunitzer, G. (1969) *Hoppe-Seyler's Z. Physiol. Chem. 350*, 1047–1066.
Aubrey, K. L., & Thomas, G. J. (1991) *Biophys. J. 60*, 1337–1349.
Blundell, T., Barlow, D., Borkarkorti, N., & Thornton, J. (1983) *Nature 306*, 281–283.
Brissette, J. L., & Russel, M. (1990) *J. Mol. Biol. 211*, 565–580.
Burley, S. K., & Petsko, G. A. (1985) *Science 229*, 23–28.
Casadevall, A., & Day, L. A. (1982) *Nucleic Acids Res. 10*, 2467–2481.
Casadevall, A., & Day, L. A. (1983) *Biochemistry 22*, 4831–4842.
Chen, A. K., & Woody, R. W. (1971) *J. Am. Chem. Soc. 93*, 29–37.
Chen, Y. H., Yang, Y. T., & Martinez, H. M. (1972) *Biochemistry 11*, 4120–4131.
Clack, B. A., & Gray, D. M. (1989) *Biopolymers 28*, 1861–1873.
Cooper, T. M., & Woody, R. W. (1990) *Biopolymers 30*, 657–676.
Creed, D. (1984) *Photochem. Photobiol. 39*, 537–562.
Cross, T. A., & Opella, S. J. (1983) *J. Am. Chem. Soc. 105*, 306–308.
Cross, T. A., & Opella, S. J. (1985) *J. Mol. Biol. 182*, 367–381.
Day, L. A. (1966) *J. Mol. Biol. 15*, 395–398.
Day, L. A. (1969) *J. Mol. Biol. 39*, 265–277.
Day, L. A., & Hoppensteadt, F. (1971) *Biopolymers 11*, 2131–2140.
Day, L. A., & Wiseman, R. L. (1978) in *The Single-Stranded DNA Phages* (Denhardt, D. T., Dressler, D., & Ray, D. S., Eds.) pp 605–625, Cold Spring Harbor Laboratories, Cold Spring Harbor, NY.
Day, L. A., Wiseman, R. L., & Marzec, C. J. (1979) *Nucleic Acids Res. 7*, 1393–1403.
Day, L. A., Marzec, C. J., Reisberg, S. A., & Casadevall, A. (1988) *Annu. Rev. Biophys. Biophys. Chem. 17*, 509–539.

Dunker, A. K., Williams, R. W., Gaber, B. P., & Peticolas, W. L. (1979a) *Biochim. Biophys. Acta 553*, 351–357.
Dunker, A. K., Williams, R. W., & Peticolas, W. L. (1979b) *J. Biol. Chem. 254*, 6444–6448.
Dunker, A. K., Fodor, P. A., & Williams, R. W. (1982) *Biophys. J. 37*, 201–203.
Dunker, A. K., Ensign, L. D., Arnold, G. E., & Roberts, L. M. (1991a) *FEBS Lett. 292*, 271–274.
Dunker, A. K., Ensign, L. D., Arnold, G. E., & Roberts, L. M. (1991b) *FEBS Lett. 292*, 275–278.
Duysens, L. N. M. (1956) *Biochim. Biophys. Acta 19*, 1–12.
Fodor, S. P. A., Dunker, A. K., Ng, Y. C., Carsten, D., & Williams, R. W. (1981) in *Bacteriophage Assembly* (DuBow, M. S., Ed.) pp 441–447, Alan R. Liss, New York.
Franconi, B., Small, E., & Peticolas, W. (1970) *J. Chem. Phys. 52*, 4369–4373.
Gall, C. M., DiVerdi, J. A., & Opella, S. J. (1981) *J. Am. Chem. Soc. 103*, 5039–5043.
Gall, C. M., Cross, T. A., DiVerdi, J. A., & Opella, S. J. (1982) *Proc. Natl. Acad. Sci. U.S.A. 79*, 101–105.
Gitter-Amir, A., Rosenheck, K., & Schneider, A. S. (1976) *Biochemistry 15*, 3131–3137.
Green, N. M., & Witkop, B. (1964) *Trans. N.Y. Acad Sci. 26*, 659–669.
Greenfield, N. J., & Fasman, G. D. (1969) *Biochemistry 8*, 4108–4116.
Griffith, J., Manning, M., & Dunn, K. (1981) *Cell 23*, 747–753.
Guy-Caffey, J. K., Rapoza, M. P., Jolley, K. A., & Webster, R. E. (1992) *J. Bacteriol. 174*, 2460–2465.
Hooker, T. M., Jr., & Schellman, J. A. (1970) *Biopolymers 9*, 1319–1348.
Hunter, G. J., Rowitch, D. H., & Perham, R. N. (1987) *Nature 327*, 252–254.
Hunter, C. A., Singh, J., & Thornton, J. M. (1991) *J. Mol. Biol. 218*, 837–846.
Krueger, W. C., & Pschigoda, L. M. (1971) *Anal. Chem. 43*, 675–677.
Kuwajima, K., Garvey, E. P., Finn, B. E., Mathews, C. R., & Sugai, S. (1991) *Biochemistry 30*, 7693–7703.
Lord, R. C., & Yu, N. T. (1970) *J. Mol. Biol. 50*, 509–524.
Makowski, L. (1984) in *Biological Macromolecules and Assemblies* (Jurnak, F. A., & McPherson, A., Eds.) Vol. 1, pp 203–253, Wiley-Interscience, New York.
Makowski, L., & Caspar, D. L. D. (1981) *J. Mol. Biol. 145*, 611–617.
Manning, M. C., & Woody, R. W. (1989) *Biochemistry 28*, 8609–8613.
Manning, M. C., & Woody, R. W. (1991) *Biopolymers 31*, 569–586.
Marvin, D. A. (1966) *J. Mol. Biol. 15*, 8–17.
Marvin, D. A. (1989) *Int. J. Biol. Macromol. 11*, 159–164.
Marvin, D. A. (1990) *Int. J. Biol. Macromol. 12*, 125–138.
Marvin, D. A., & Wachtel, E. J. (1975) *Nature (London) 253*, 19–23.
Marvin, D. A., & Wachtel, E. J. (1976) *Philos. Trans. R. Soc. London, B 276*, 81–98.
Marvin, D. A., Pigram, W. J., Wiseman, R. L., Wachtel, E. J., & Marvin, F. J. (1974) *J. Mol. Biol. 88*, 581–600.
Marzec, C. J., & Day, L. A. (1988) *Biophys. J. 53*, 425–440.
Model, P., & Russel, M. (1988) in *The Bacteriophages* (Calendar, R., Ed.) pp 375–456, Plenum, New York.
Nakashima, Y., & Konigsberg, W. H. (1974) *J. Mol. Biol. 88*, 598–602.
Newman, J., Swinney, H. L., & Day, L. A. (1977) *J. Mol. Biol. 116*, 593–603.
Ng, Y. C., & Dunker, A. K. (1981) *Prog. Clin. Biol. Res. 64*, 467–474.
Nozaki, Y., Reynolds, J. A., & Tanford, C. (1978) *Biochemistry 17*, 1239–1246.
Opella, S. J., Stewart, P. L., & Valentine, K. G. (1987) *Q. Rev. Biophys. 19*, 1–49.
Patchornik, A., Lawson, W. B., & Witkop, B. (1958) *J. Am. Chem. Soc. 80*, 4747–4748.
Quadrifoglio, F., & Urry, D. W. (1968) *J. Am. Chem. Soc. 90*, 2755–2761.
Rasched, I., & Oberer, E. (1986) *Microbiol. Rev. 50*, 401–427.
Ray, C. R. (1975) in *Advanced Engineering Mathematics* (Arthur, A. A., & LaBarbera, M., Eds.) 4th ed., pp 129–131, MeGraw-Hill, New York.
Reisberg, S. A. (1989) Ph.D. Thesis, New York University.
Rohrer, J., & Kuhn, A. (1990) *Science 250*, 1418–1421.
Russel, M. (1991) *Mol. Microbiol. 5*, 1607–1613.
Savitisky, & Golay (1967) *Anal. Chem. 36*, 1627–1639.
Schmidt, H., & Bieker, L. (1979) *Arch. Biochem. Biophys. 195*, 205–210.
Schneider, A. S., Schneider, M. J., & Rosenheck, K. (1979) *Proc. Natl. Acad. Sci. U.S.A. 66*, 793–798.
Singh, J., & Thornton, J. M. (1985) *FEBS Lett. 191*, 1–6.
Smilowitz, H. (1974) *J. Virol. 13*, 94–99.
Spande, T. F., & Witkop, B. (1967) *Methods Enzymol. 11*, 506–522.
Tanford, C., & Reynolds, J. A. (1976) *Biochim. Biophys. Acta 457*, 133–170.
Thomas, G. J., Jr. (1987) in *Biological Applications of Raman Spectroscopy* (Spiro, T. G., Ed.) Vol. 1, pp 135–201, Wiley-Interscience, New York.
Thomas, G. J., Jr., & Murphy, P. (1975) *Science 188*, 1205–1207.
Thomas, G. J., Jr., & Day, L. A. (1981) *Proc. Natl. Acad. Sci. U.S.A. 78*, 2962–2966.
Thomas, G. J., Jr., Prescott, B., & Day, L. A. (1983) *J. Mol. Biol. 165*, 321–356.
Tinoco, I., Woody, R. W., & Bradley, D. F. (1963) *J. Chem. Phys. 38*, 1317–1325.
Tinoco, I., Jr., Bustamante, C., & Maestre, M. F. (1980) *Annu. Rev. Biophys. Bioeng. 9*, 107–141.
Tinoco, I., Jr., Mickols, W., Maestre, M. F., & Bustamante, C. (1987) *Annu. Rev. Biophys. Bioeng. 16*, 319–349.
Warme, P. K., & Morgan, R. S. (1978) *J. Mol. Biol. 118*, 289–304.
Webster, R. D., & Lopez, J. (1985) in *Virus Structure and Assembly* (Casjens, S., Ed.) pp 235–267, Jones & Bartlett, Boston.
Williams, R. W., & Dunker, A. K. (1977) *J. Biol. Chem. 252*, 6253–6255.
Williams, R. W., & Dunker, A. K. (1981) *J. Mol. Biol. 152*, 783–813.
Williams, R. W., Dunker, A. K., & Peticolas, W. L. (1984) *Biochim. Biophys. Acta 791*, 131–144.
Woody, R. W. (1985) *Peptides (Fayetteville, N.Y.) 7*, 15–114.